REPORT

TROPICAL FORESTS

Demographic trade-offs predict tropical forest dynamics

Nadja Rüger[1,2,3]*, Richard Condit[4,5], Daisy H. Dent[3,6], Saara J. DeWalt[7], Stephen P. Hubbell[3,8], Jeremy W. Lichstein[9], Omar R. Lopez[3,10], Christian Wirth[1,11,12], Caroline E. Farrior[13]

Understanding tropical forest dynamics and planning for their sustainable management require efficient, yet accurate, predictions of the joint dynamics of hundreds of tree species. With increasing information on tropical tree life histories, our predictive understanding is no longer limited by species data but by the ability of existing models to make use of it. Using a demographic forest model, we show that the basal area and compositional changes during forest succession in a neotropical forest can be accurately predicted by representing tropical tree diversity (hundreds of species) with only five functional groups spanning two essential trade-offs—the growth-survival and stature-recruitment trade-offs. This data-driven modeling framework substantially improves our ability to predict consequences of anthropogenic impacts on tropical forests.

Tropical forests are highly dynamic. Only about 50% of the world's tropical forests are undisturbed old-growth forests (*1*). The remaining half comprises forests regenerating after previous land use, timber or fuelwood extraction, or natural disturbances. Even unmanaged old-growth forests are a dynamic mosaic of patches recovering from single or multiple treefall gaps (*2*). Thus, understanding how forest structure and composition of the diverse tree flora change during recovery from disturbance is fundamental to predicting carbon dynamics, as well as to planning sustainable forest management (*3*). Despite the importance of regenerating tropical forests for the global carbon cycle and timber industry, our mechanistic understanding and ability to forecast compositional changes of these forests remain severely limited (*4*).

Conceptually, tropical forest succession has been viewed mostly through a one-dimensional lens distinguishing species along a fast-slow life-history continuum, or growth-survival tradeoff (*4*–*6*). "Fast" species are light-demanding and grow quickly, but survive poorly, and dominate early successional stages, whereas "slow" species are shade-tolerant and grow slowly, but survive well, and reach dominance in later successional stages. However, several studies suggest that tropical tree communities are also structured along a second major trade-off axis that is orthogonal to the growth-survival tradeoff: the stature-recruitment trade-off (*7*, *8*). The stature-recruitment trade-off distinguishes long-lived pioneers (LLPs) from short-lived breeders (SLBs). LLPs grow fast and live long, and hence attain a large stature, but exhibit low recruitment. SLBs grow and survive poorly, and hence remain short-statured, but produce large numbers of offspring (*8*). However, we are lacking a systematic assessment of how important these trade-offs are for tropical forest dynamics.

To evaluate the importance of the growth-survival and stature-recruitment trade-offs for tropical forest dynamics, we parameterized the perfect plasticity approximation (PPA) model (*9*, *10*) with demographic trade-offs derived from forest inventory data. The PPA model simulates the dynamics of a potentially large number of species based on a small set of demographic rates (growth, survival, and recruitment) and accounts for height-structured competition for light by distinguishing up to four canopy layers (*11*). Canopy gaps are filled by the tallest trees from lower canopy layers, without regard for their horizontal position [perfect plasticity assumption (*9*)].

Our study site is the tropical moist forest at Barro Colorado Island (BCI), Panama, where recruitment, growth, and survival of individual trees have been monitored in a 50-ha plot for more than 30 years (*2*, *11*, *12*). To account for the dependence of these demographic rates on light availability, we assigned all monitored individuals of 282 tree and shrub species to one of four canopy layers on the basis of their size and the size of their neighbors (*11*, *13*) and estimated model parameters (annual diameter growth and survival rates) for each species in each canopy layer (*8*). Additionally, we calculated species recruitment rates per unit of basal area. A dimension reduction of model parameters [weighted principal components analysis (PCA) (*14*)] reveals the two demographic trade-offs, that is, the growth-survival trade-off and the stature-recruitment trade-off, which together explain 65% of demographic variation among the 282 species (Fig. 1).

Our goal here is to explore whether this low-dimensional demographic trade-off space can capture tropical forest dynamics, and if so, how much demographic diversity is necessary to accurately predict changes in basal area (a proxy for carbon storage in aboveground biomass) over time. We used species' positions in the trade-off space to estimate model parameters for all 282 species (*11*), thus smoothing

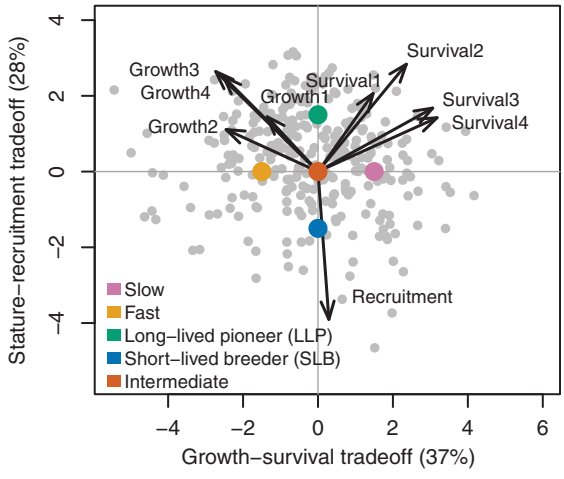

Fig. 1. Demographic trade-offs for 282 tree species at BCI, Panama. Arrows show loadings of a weighted PCA on annual diameter growth and survival rates of individuals ≥1 cm in diameter in four canopy layers (where Growth1 indicates growth in full sun and Growth4 indicates growth of individuals that are shaded by three canopy layers) and the number of sapling recruits per unit of basal area. Colored dots are locations in demographic space of plant functional types (PFTs) that were used in model scenarios 1 and 3.

[1]German Centre for Integrative Biodiversity Research (iDiv) Halle-Jena-Leipzig, Deutscher Platz 5e, 04103 Leipzig, Germany. [2]Department of Economics, University of Leipzig, Grimmaische Straße 12, 04109 Leipzig, Germany. [3]Smithsonian Tropical Research Institute, Apartado 0843-03092, Balboa, Ancón, Panama. [4]Field Museum of Natural History, 1400 S. Lake Shore Dr., Chicago, IL 60605, USA. [5]Morton Arboretum, 4100 Illinois Rte. 53, Lisle, IL 60532, USA. [6]Biological and Environmental Sciences, University of Stirling, Stirling FK9 4LA, UK. [7]Department of Biological Sciences, Clemson University, Clemson, SC 29634, USA. [8]Department of Ecology and Evolutionary Biology, University of California, Los Angeles, CA 90095, USA. [9]Department of Biology, University of Florida, Gainesville, FL 32611, USA. [10]Instituto de Investigaciones Científicas y Servicios de Alta Tecnología (INDICASAT), Edificio 209, Clayton, Panama. [11]Systematic Botany and Functional Biodiversity, Institute of Biology, University of Leipzig, Johannisallee 21-23, 04103 Leipzig, Germany. [12]Max Planck Institute for Biogeochemistry, Hans-Knöll Str. 10, 07745 Jena, Germany. [13]Department of Integrative Biology, University of Texas at Austin, Austin, TX 78712, USA.
*Corresponding author. Email: nadja.rueger@idiv.de

across observed relationships between demographic rates. We simulated forest dynamics under four scenarios that differed in the number of trade-offs (one versus two) and level of demographic diversity [number of simulated species or plant functional types (PFTs); Table 1 and Fig. 2A]. We tested model performance for the 50-ha old-growth plot at BCI (also used to derive demographic rates) and for a chronosequence of nearby secondary forests that share a similar topography and soil and a majority of tree species (*15*).

To compare the observed dynamics of the 50-ha old-growth plot in BCI with model predictions, we initialized the model with inventory data from 1985 and simulated forest dynamics until 2010. When only the growth-survival trade-off was included, basal area was predicted to decline because of a decline in the number of trees >20 cm in diameter, especially of fast species (Fig. 2B and fig. S1). Including the stature-recruitment trade-off improved the match between predicted and observed basal area and aboveground biomass (AGB; Fig. 2B and figs. S2 and S3) for different PFTs and size classes (figs. S4 and S5). However, when all species were simulated individually (scenario 4), the number of large trees (>60 cm in diameter) and basal area were incorrectly predicted to increase (fig. S1). This was attributable to the greater influence of measurement errors due to small sample sizes when parameterizing the model for 282 species (*11*), although most species-level predictions were reliable (fig. S6). Maximum diameters were accurately predicted by all scenarios, except for scenario 2, where observed maximum diameters >150 cm were not reproduced (fig. S7). This test shows that the model scenarios that included both trade-offs were able to reproduce the structure and stability of the forest over the time span that was used to derive demographic rates.

Next, we tested the ability of the model to predict successional changes in secondary forests. We used the same model parameterization scenarios, initialized the model with data from 40-year-old secondary forest, and compared predictions of forest dynamics with observations from a chronosequence of 60-, 90-, and 120-year-old secondary forests (two 1-ha plots in each age class). As in old-growth forest, predictions of secondary succession were most accurate when forest diversity was represented by five PFTs spanning both demographic trade-offs. When only the growth-survival trade-off was included, the increase of basal area (Fig. 2C) and AGB (fig. S2) during succession was underestimated because the number of large trees (>60 cm in diameter) was underestimated

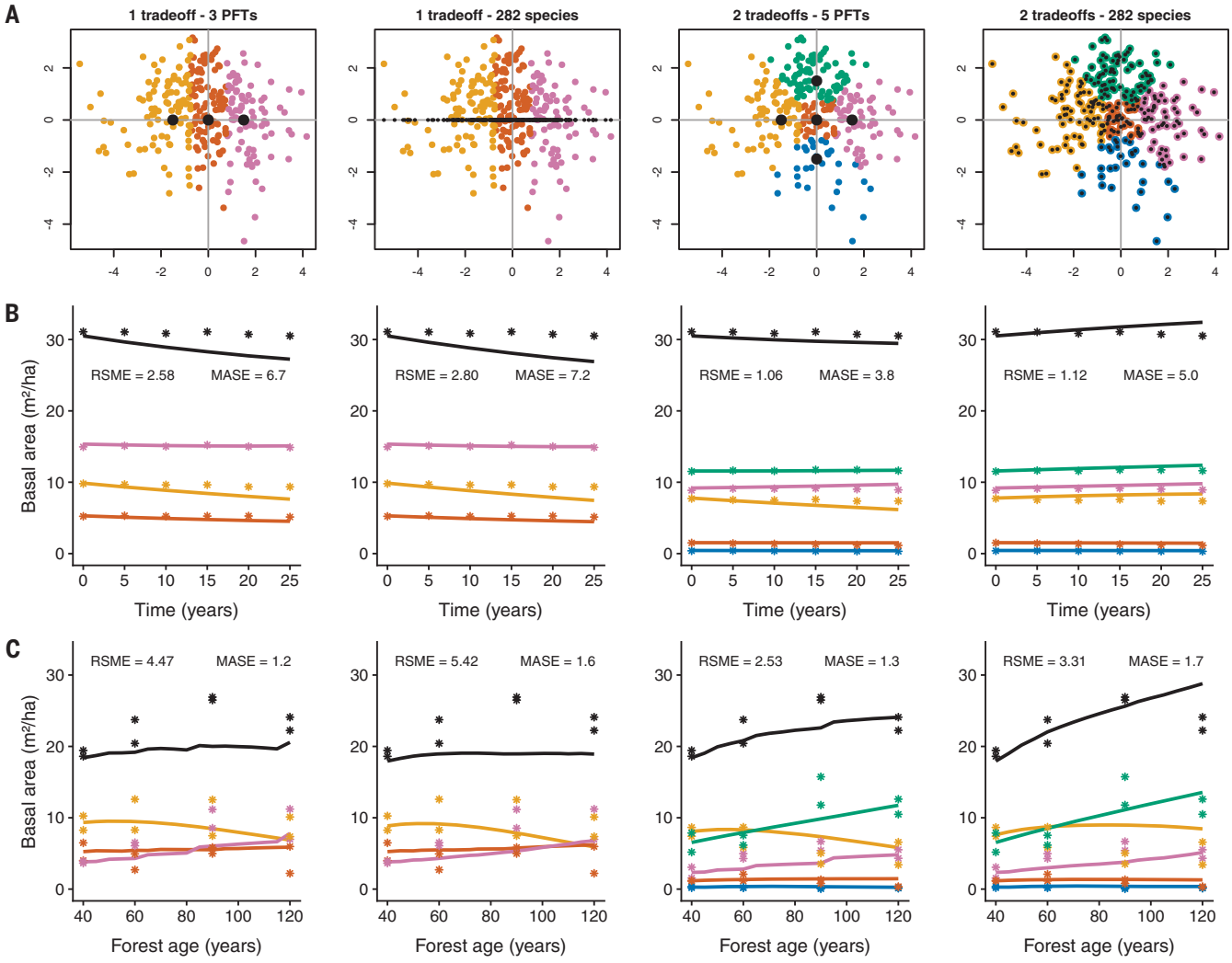

Fig. 2. Predicted and observed basal area in four model scenarios. Model scenarios are shown in Table 1. (**A**) Locations of species (colored dots) and representative PFTs used for model scenarios (black dots) in demographic space; each species was assigned to a PFT on the basis of proximity in demographic space and color coded as in Fig. 1. (**B** and **C**) Predicted (lines) and observed (asterisks) basal area by PFT in old-growth tropical forest (BCI; black is total basal area) (B) and secondary tropical forest in the Barro Colorado Nature Monument (C). RSME is the root mean square error of prediction of total basal area, and MASE is the mean absolute scaled error of PFT-level predictions (*11*). Lines and asterisks are color coded as in Fig. 1.

(fig. S8). By contrast, when both trade-offs were included, observed successional changes in basal area, AGB, and abundance for different PFTs and size classes were accurately reproduced (Fig. 2C and figs. S2 and S8 to S10). However, when all species were simulated individually (scenario 4), the number of large trees (>60 cm in diameter) and basal area of fast species and LLPs were overestimated. The observed peak in basal area in the 90-year-old secondary forest is likely caused by remnant trees in the study plots and disappears when larger spatial scales are considered (*16*). The diameter distribution after 400 years of simulation closely matched the observed diameter distribution only when both demographic trade-offs were included (Fig. 3A).

In addition to the above simulations, we also ran simulations with alternative initial conditions to explore the robustness of our results. The alternative initial conditions [bare ground and 20-year-old forest; (*11*)] did not qualitatively affect our results. For all initial conditions, the five-PFT scenario spanning both demographic trade-offs yielded predictions that best matched observations (fig. S11). Together, the old-growth and secondary forest simulations suggest a close match between the five-PFT scenario and the available data. However, even with this multidecadal dataset, we have only a limited capacity to rigorously test a forest dynamics model. For example, we used chronosequence data to represent the first 120 years of secondary succession because no time series of direct observations of succession exists for such a long period.

To assess whether the forest in the 50-ha plot at BCI is at equilibrium with the local disturbance regime, we simulated forest succession (starting from 40 years as above) under scenario 3 for 1000 years without any external disturbances. Here, the slow and LLP PFTs codominated the forest after 400 to 500 years (fig. S12). The fast PFT died out because the canopy gaps that it requires for persistence (*17*) are treated in our model in a simplistic (non–spatially explicit) manner. In reality, however, the forest is composed of a mosaic of patches of different successional age since the last disturbance event (*18*). Thus, we compared the simulated successional trajectories of the fast and slow PFTs with observed species composition at the 0.1-ha scale to infer the patch-scale age distribution [fig. S13; (*11*)]. This model-inferred age distribution suggests that the majority of the 0.1-ha patches within the BCI 50-ha plot are between 50 and 250 years old. This is consistent with light detection and ranging (LIDAR) data collected on BCI, which suggest that between 0.43 and 1.6% of the area is disturbed every year, corresponding to an average disturbance interval between 63 and 233 years (*11*, *19*). When we use the estimated proportion of 0.1-ha patches in each age class to generate the PFT composition at equilibrium with the disturbance regime, predictions closely match observations (Fig. 3B).

These results suggest that the forest in the 50-ha plot at BCI is at equilibrium with the local disturbance regime. This helps to resolve a long-standing dispute of whether LLPs are a transient feature of successional forests (*5*, *20*, *21*) and shows that, in this forest, they are not transient but an integral and dominant component of the old-growth forest. Indeed, LLPs dominate most successional stages and contribute more AGB than any other demographic group, except in very young forests (<40 years) or patches that have remained undisturbed for a long time (>400 years, fig. S12). They can maintain populations in the absence of large-scale disturbances and compensate for their low recruitment by growing quickly up to the canopy or emergent layer, where they may persist as a seed source for several centuries (*8*).

Overall, our results suggest that two demographic trade-offs are needed to accurately predict successional patterns in tropical forest structure and composition. Considering only the fast-slow continuum of life histories is not sufficient because it ignores LLPs, one of the most important (in terms of tree size and AGB) components in many tropical forests. Although the existence of LLPs has long been recognized (*4*), they have often been assumed to be part of the fast-slow continuum—that is, considered to be midsuccessional—because they reach their highest basal area in intermediate stages of succession (*5*). However, LLPs lie on a second demographic dimension (*8*, *22*), and this second dimension is essential to understanding tropical forest dynamics.

Our results also suggest that a small number of demographic niches is sufficient to capture the dynamics of the BCI forest. Specifically, just five PFTs were sufficient to adequately capture successional patterns of forest composition and carbon dynamics (Figs. 2 and 3). To explore the robustness of the five-PFT approach under future climate, we used relationships between climate, functional traits, and demographic rates to implement our model simulations under alternative future climate scenarios (*11*). As under current conditions, the five-PFT and species-level models yielded similar predictions to each other under future climate scenarios (fig. S14), suggesting that a limited number of PFTs may be sufficient to capture the community response to climate change. This conclusion warrants further investigation with models that include physiological mechanisms not included in our model, as well as additional functional axes (e.g., drought tolerance) that are likely to be relevant at broader spatial or temporal scales. Nevertheless, our results suggest that functional

Table 1. Model scenarios. Model scenarios differ in the number of included trade-offs and the level of demographic diversity.

Scenario	Trade-offs	Demographic diversity
1	Growth-survival	Three PFTs (fast, intermediate, slow)
2	Growth-survival	282 species
3	Growth-survival, stature-recruitment	Five PFTs (fast, slow, LLP, SLB, intermediate)
4	Growth-survival, stature-recruitment	282 species

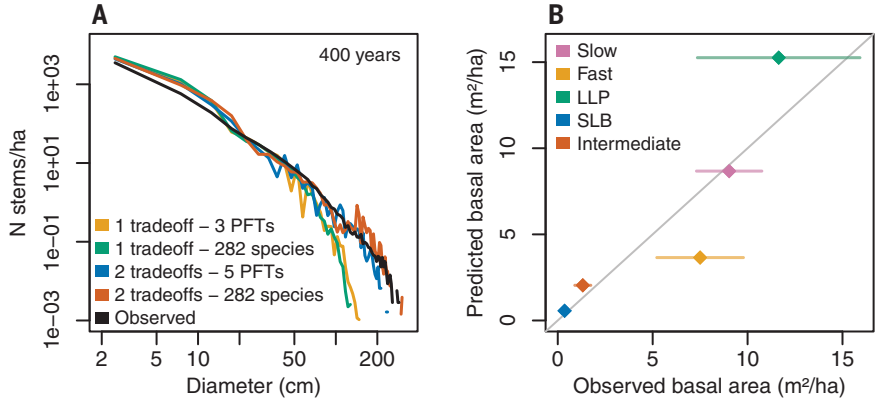

Fig. 3. Model validation. (**A**) Diameter distribution in 400-year-old simulated forest for the four model scenarios shown in Table 1. N stems, number of stems. (**B**) Predicted and observed basal area in model scenario 3. Observed basal area is from an old-growth tropical forest in BCI, Panama. Predicted basal area is based on the estimated number of 0.1-ha patches in each age class [fig. S13; (*11*)].

diversity in species-rich tropical forests may be much smaller than taxonomic diversity and that tropical forest diversity could be accurately represented in Earth system models by a small number of PFTs that span the relevant functional axes (*23*).

Beyond suggesting a simple yet accurate means to represent tropical forest functional diversity with a limited number of PFTs, our study also demonstrates the feasibility of embracing species-level diversity. Together, the demographic forest model and the empirical demographic trade-offs define an objective and reproducible workflow that also delivers stable predictions of forest dynamics when run at the species level. Such workflows, along with the increasing availability of tropical forest inventory data, offer the opportunity to develop truly species-based models to support the evidence-based planning of forest restoration and sustainable tropical forest management by predicting rates and trajectories of forest regrowth at both the species and community levels (*3*).

REFERENCES AND NOTES

1. Food and Agriculture Organization of the United Nations (FAO), "Global Forest Resources Assessment 2010" (FAO Forestry Paper 163, FAO, 2010).
2. S. P. Hubbell *et al*., *Science* **283**, 554–557 (1999).
3. E. Rutishauser *et al*., *Curr. Biol.* **25**, R787–R788 (2015).
4. R. L. Chazdon, *Second Growth: The Promise of Tropical Forest Regeneration in an Age of Deforestation* (Univ. Chicago Press, 2014).
5. B. Finegan, *Trends Ecol. Evol.* **11**, 119–124 (1996).
6. P. B. Reich, *J. Ecol.* **102**, 275–301 (2014).
7. T. Kohyama, E. Suzuki, T. Partomihardjo, T. Yamada, T. Kubo, *J. Ecol.* **91**, 797–806 (2003).
8. N. Rüger *et al*., *Ecol. Lett.* **21**, 1075–1084 (2018).
9. N. Strigul, D. Pristinski, D. Purves, J. Dushoff, S. Pacala, *Ecol. Monogr.* **78**, 523–545 (2008).
10. D. W. Purves, J. W. Lichstein, N. Strigul, S. W. Pacala, *Proc. Natl. Acad. Sci. U.S.A.* **105**, 17018–17022 (2008).
11. Materials and methods are available as supplementary materials.
12. R. Condit, *Tropical Forest Census Plots* (Environmental Intelligence Unit Series, Springer, 1998).
13. S. Bohlman, S. Pacala, *J. Ecol.* **100**, 508–518 (2012).
14. L. Delchambre, *Mon. Not. R. Astron. Soc.* **446**, 3545–3555 (2014).
15. J. S. Denslow, S. Guzman, *J. Veg. Sci.* **11**, 201–212 (2000).
16. J. Mascaro, G. P. Asner, D. H. Dent, S. J. DeWalt, J. S. Denslow, *For. Ecol. Manage.* **276**, 62–70 (2012).
17. M. D. Swaine, T. C. Whitmore, *Vegetatio* **75**, 81–86 (1988).
18. J. Q. Chambers *et al*., *Proc. Natl. Acad. Sci. U.S.A.* **110**, 3949–3954 (2013).
19. E. Lobo, J. W. Dalling, *Proc. R. Soc. London Ser. B* **281**, 20133218 (2014).
20. R. Condit, R. Sukumar, S. P. Hubbell, R. B. Foster, *Am. Nat.* **152**, 495–509 (1998).
21. D. Sheil, D. F. R. P. Burslem, *Trends Ecol. Evol.* **18**, 18–26 (2003).
22. I. M. Turner, *The Ecology of Trees in the Tropical Rain Forest* (Cambridge Univ. Press, 2001).
23. D. Purves, S. Pacala, *Science* **320**, 1452–1453 (2008).
24. R. Condit *et al*., Barro Colorado Forest Census Plot Data, 2012 Version, Center for Tropical Forest Science Databases, DSpace Repository (2012); doi:10.5479/data.bci.20130603.
25. C. Farrior, cfarrior/Ruger_etal_2020: Ruger_etal_2020, Zenodo (2020); doi:10.5281/zenodo.3688497.

ACKNOWLEDGMENTS

We thank D. Purves for sharing the PPA model code; S. Bohlman for sharing allometry data; A. Gentile for downloading climate data; S. Bohlman, H. Muller-Landau, S. Pacala, and D. Purves for inspiring discussions and helpful suggestions; and two anonymous reviewers for constructive criticism. **Funding:** N.R. was funded by a research grant from Deutsche Forschungsgemeinschaft DFG (RU 1536/3-1). N.R., C.W., and J.W.L. (sDiv sabbatical fellowship) acknowledge the support of the German Centre for Integrative Biodiversity Research (iDiv) funded by Deutsche Forschungsgemeinschaft DFG (FZT 118). The BCI forest dynamics research project was founded by S. P. Hubbell and R. B. Foster and is now managed by R. Condit, S. Lao, and R. Perez under the Center for Tropical Forest Science and Smithsonian Tropical Research Institute in Panama. Numerous organizations have provided funding, principally the U.S. National Science Foundation, and hundreds of field workers have contributed. The secondary forest data collection was funded by a grant from SENACYT (COL10-052) to D.H.D., S.J.D., and O.R.L. **Author contributions:** N.R. designed the research with input from C.E.F., J.W.L., and C.W.; N.R. and C.E.F. performed the research; R.C., D.H.D., S.J.D., S.P.H., and O.R.L. provided forest inventory data; N.R. wrote the first draft of the manuscript with contributions from C.E.F., J.W.L., and C.W.; and all authors contributed to subsequent versions of the paper. **Competing interests:** The authors declare no competing interests. **Data and materials availability:** Forest inventory data are publicly available at DSpace Repository [old-growth forest (*24*)] and DataSTORRE (secondary forest, http://hdl.handle.net/11667/144). The model code is available on GitHub (https://github.com/cfarrior/Ruger_etal_2020) and archived at Zenodo (*25*).

SUPPLEMENTARY MATERIALS

science.sciencemag.org/content/368/6487/165/suppl/DC1
Materials and Methods
Figs. S1 to S15
Tables S1 to S8
References (*26*–*40*)
Data S1 and S2

View/request a protocol for this paper from *Bio-protocol*.

12 September 2019; accepted 27 February 2020
10.1126/science.aaz4797